

# Single-pixel complex-field imaging through scattering media

YINING HAO<sup>1</sup> AND WEN CHEN<sup>1,2,\*</sup>

<sup>1</sup>*Department of Electrical and Electronic Engineering, The Hong Kong Polytechnic University, Hong Kong, China*

<sup>2</sup>*Photonics Research Institute, The Hong Kong Polytechnic University, Hong Kong, China*

\*[owen.chen@polyu.edu.hk](mailto:owen.chen@polyu.edu.hk)

---

**Much research in optics was conducted to retrieve phase of the light field, e.g., via a reference wave (such as holography) or single-path optical diffraction. However, it is well recognized that a complete application of complex-field imaging (i.e., amplitude and phase) is still restricted by the existence of scattering media. In this Letter, we report high-resolution complex-field imaging with single-pixel detection which can effectively suppress scattering effect. Complex fields are retrieved by using a series of collected single-pixel light intensities with an alternating projection (AP) method. A momentum and the denoising engine are integrated into the iterative process to increase convergence speed and reduce sampling ratios with quality enhancement of the retrieved complex fields. A series of optical experiments are designed and conducted, and it is experimentally demonstrated that the retrieved complex fields related to the object are of high quality. The proposed method could open an avenue for a wide range of applications related to complex-field imaging through scattering media.**

---

The light field can oscillate at exceedingly high frequencies in the order of petahertz [1]. The rapid oscillation leads to an impossible task to precisely detect light fields. The sensors used in an imaging system measure photon flux which is directly related to amplitude of the light fields, and amplitude information concerning the relative brightness of different positions can be captured. The phase information that reveals details about the variation of spatial structure in the wavefront cannot be captured, but is crucial for a wide range of applications, such as biological [2], astronomy [3] and crystallography [4]. Additional strategies, either physical or

algorithmic, need to be incorporated into optical systems to retrieve the lost phase. For instance, holographic imaging is developed to reconstruct complex amplitude by interfering the light field carrying target information with a reference so that additional information is introduced during the recording [5]. Alternatively, coherent diffractive imaging [6] was developed to reconstruct a complex field from the recorded far-field diffraction patterns using specially-designed phase retrieval algorithms. Although different approaches have been developed to realize complex-field reconstruction in different regimes, there are still obstacles that restrict the applications of complex-field imaging. Among them, a challenge remains on how to reconstruct high-quality complex fields through scattering media. The inhomogeneity of scattering media causes light fields to be scattered into various paths, leading to the generation of speckle patterns in the detection plane [7]. The broken mapping relationship indicated by speckle patterns poses a challenge for phase retrieval. To realize imaging through scattering media, different approaches are studied, such as wavefront shaping [8], adaptive optics [9] and speckle correlation [10]. However, most methods are designed to recover amplitude patterns, and phase retrieval is still restricted by the existence of scattering media. Therefore, it is meaningful to extend the studies on optical imaging through scattering media to complex-field imaging with novel strategies.

In recent years, single-pixel imaging (SPI) [11] has emerged as a promising approach to recover spatial information of a target from a series of single-pixel light intensities collected by a single-pixel bucket detector. In SPI, optical wave is modulated by a series of known patterns, creating a correlated relationship between the illumination patterns and single-pixel light intensities. Since single-pixel intensity measurements can be interpreted from different perspectives, various reconstruction methods have been developed to achieve an enhanced signal-to-noise ratio (SNR) and a reduced sampling ratio [12,13]. With a rapid development of SPI,

it has been widely applied, e.g., optical transmission [14], optical encryption [15] and terahertz imaging [16]. In particular, SPI through scattering media has been explored [17] for the recovery of amplitude information of an object.

In this Letter, we report a novel alternating projection (AP) method for single-pixel complex-field imaging through scattering media. By interpreting each collected single-pixel light intensity as a zero-frequency component of Fourier spectrum, the AP [18] is integrated into complex-field reconstruction. Therefore, superior performance of SPI can be leveraged for complex-field imaging through scattering media. A momentum and the denoising engine are adopted in the proposed complex-field reconstruction algorithm, and the problem of slow convergence speed in conventional AP is effectively addressed. The number of measurements is also reduced, and reconstruction quality can be enhanced. A series of optical experiments are designed and conducted, and experimental results demonstrate that the proposed method is feasible and effective to retrieve high-quality complex fields through scattering media.

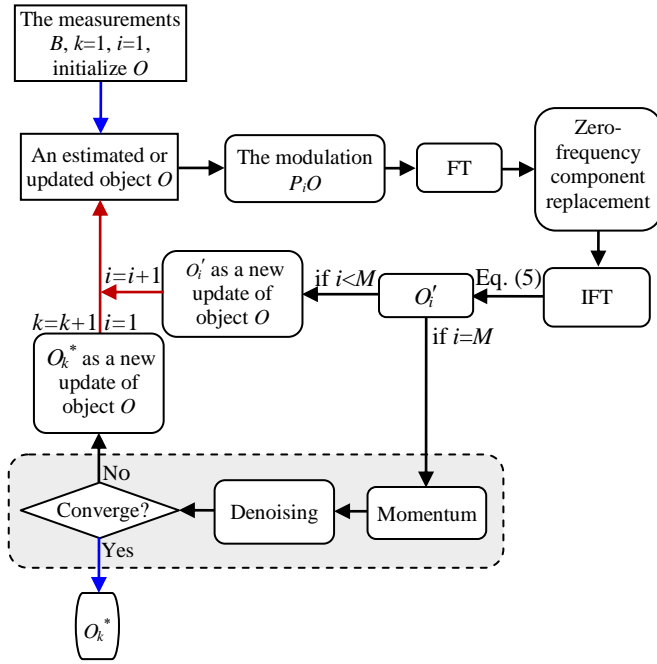


**Fig. 1.** A block diagram of the proposed algorithm for retrieving the complex fields related to object:  $O^*$ , an estimate of the complex field related to object;  $M$ , the total number of measurements (realizations); FT, Fourier transform; IFT, inverse Fourier transform;  $k$ , the number of iterations (1,2,3,...);  $i=1,2,3,\dots,M$ .

In SPI through scattering media, a phase retrieval algorithm based on AP is developed to retrieve the complex field via applying constraints in two planes, i.e., the image and Fourier planes. To apply AP, the constraint used in the Fourier plane is modified to keep the consistency with the collected single-pixel light intensities. This is conducted based on the properties of Fourier transform [19]. The single-pixel measurement corresponding to each

illumination pattern is considered as a constraint to process zero-frequency component of Fourier spectrum, and can be described by

$$B_i = \left| \iint P_i(x, y) O(x, y) e^{-j2\pi(ux+vy)} dx dy \Big|_{u=0, v=0} \right|^2, \quad (1)$$

where  $B_i$  denotes the  $i$ th single-pixel measurement (realization),  $||$  denotes a modulus operation,  $j = \sqrt{-1}$ , and  $P_i$  denotes the  $i$ th illumination pattern.

To retrieve a complex field with  $n \times n$  pixels, complex amplitude of the object is first initialized. With an illumination pattern  $P_i \in \mathbb{R}^{n \times n}$ , wave modulation can be described by

$$\varphi_i = P_i O. \quad (2)$$

Then, Fourier transform is applied, and a constraint is applied to the spectrum.

$$\Phi_i = \mathcal{F}(\varphi_i), \quad (3)$$

where  $\mathcal{F}$  denotes Fourier transform. The magnitude of zero-frequency component of  $\Phi_i$  is replaced by  $\sqrt{B_i}$ , and the updated spectrum can be described by

$$\Phi'_i(u, v) = \begin{cases} \sqrt{B_i} \frac{\Phi_i(u, v)}{|\Phi_i(u, v)|}, & (u=0, v=0) \\ \Phi_i(u, v), & \text{others} \end{cases}. \quad (4)$$

A complex field in the image plane is further obtained via inverse Fourier transform ( $\mathcal{F}^{-1}$ ) of  $\Phi'_i$ . Here, the AP is designed and used, and the expected update of the object is conducted by applying the constraints in image and Fourier planes. The updated complex field related to the object can be described by

$$O'_i = \arg \min_o \|\mathcal{F}^{-1}(\Phi'_i) - P_i O\|^2. \quad (5)$$

After all the collected single-pixel light intensities are processed using the aforementioned method, a momentum and the denoising engine are flexibly applied as shown in Fig. 1. The momentum [20] and denoising engines (see Section 1 in Supplement 1) are adapted to the iterative process to enhance the convergence speed and reduce the number of measurements with an enhancement of reconstruction quality. Specifically, the momentum-accelerated algorithm can efficiently avoid small local minima, leading to the faster convergence speed. Integrating a denoising engine into the proposed algorithm can allow the usage of *prior* knowledge, thereby enhancing quality of the reconstructed object images. The above steps are repeated until a preset condition, i.e., mean squared error (MSE), is satisfied.

Optical experiments are conducted to show feasibility and effectiveness of the proposed single-pixel complex-field imaging through scattering media, and a schematic of the optical setup is shown in Fig. 2. A green laser is used as light source with a maximum power of 200.0 mW and wavelength of 532.0 nm. Random patterns with a uniform distribution are displayed by an amplitude-only spatial light modulator (SLM, Holoeye HED 6001)

with pixel size of  $8.0\ \mu\text{m}$ , and are sequentially projected onto the object via a 4f structure. The focal lengths of lenses  $L_2$  and  $L_3$  are  $50.0\ \text{mm}$  and  $150.0\ \text{mm}$ , respectively. The exit wave after the object propagates through scattering media. Finally, the scattered wave is collected into a single-pixel photodetector (Thorlabs, PDA100A2) via a lens and an aperture (size of  $5.0\ \mu\text{m}$ ), i.e., a sequence of single-pixel light intensities to be recorded.

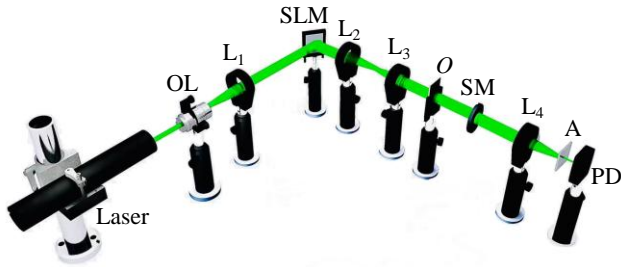


**Fig. 2.** A schematic optical setup: OL, Objective lens; SLM, spatial light modulator;  $L_1$ – $L_4$ , lens;  $O$ , an object to be tested; SM, scattering media; A, aperture; PD, a single-pixel photodetector.

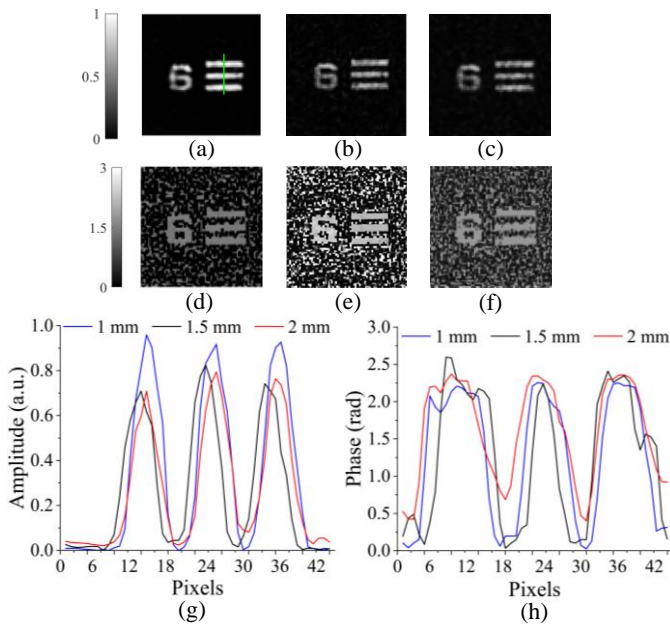


**Fig. 3.** The reconstructed amplitude patterns through polypropylene sheets with thickness of (a)  $1\ \text{mm}$ , (b)  $1.5\ \text{mm}$  and (c)  $2\ \text{mm}$ ; the retrieved phase patterns through polypropylene sheets with thickness of (d)  $1\ \text{mm}$ , (e)  $1.5\ \text{mm}$  and (f)  $2\ \text{mm}$ ; (g) and (h) the profiles along the line (indicated in (a)) respectively in the reconstructed amplitude patterns and the retrieved phase patterns.

Figure 3 shows the retrieved complex fields, when SPI through frosted translucent polypropylene sheets with thickness of  $1\ \text{mm}$ ,  $1.5\ \text{mm}$  and  $2\ \text{mm}$  is respectively conducted. The Group 2 Element 6 of USAF 1951 resolution target is tested. As can be seen in the retrieved amplitude and phase patterns, the proposed method can effectively withstand scattering to realize high-quality complex-

field imaging. The pixels along the line (indicated in Fig. 3(a)) of the retrieved amplitude and phase patterns are shown in Figs. 3(g) and 3(h), respectively. The peaks can be clearly distinguished in the reconstructed amplitude and phase patterns. The Group 2 Element 6 of USAF 1951 resolution target is resolved by using the proposed method, i.e., spatial resolution of  $140.3\ \mu\text{m}$ . Contrast-to-noise ratio (CNR) [21–24] is also calculated to quantitatively evaluate quality of the reconstructed object (see Fig. S1 in Supplement 1). The CNRs of amplitude patterns in Figs. 3(a)–3(c) are  $15.13$ ,  $9.53$  and  $7.35$ , respectively. It is indicated that high-quality complex-field reconstruction is realized by using the proposed method in scattering environments.

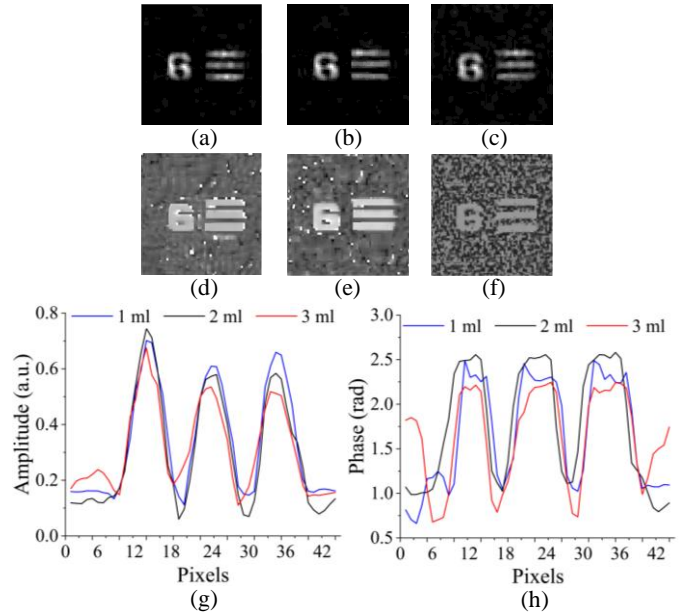
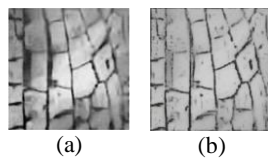


**Fig. 4.** The reconstructed amplitude patterns through turbid water with milk of (a)  $1\ \text{ml}$ , (b)  $2\ \text{ml}$  and (c)  $3\ \text{ml}$ ; the retrieved phase patterns through turbid water with milk of (d)  $1\ \text{ml}$ , (e)  $2\ \text{ml}$  and (f)  $3\ \text{ml}$ ; and (g) and (h) the profiles along the line (indicated in Fig. 3(a)) respectively in the reconstructed amplitude patterns and the retrieved phase patterns.

To show the proposed method, an environment with turbid water is also designed and applied in Fig. 2. A transparent water tank with dimensions of  $5.0\ \text{cm}$  (length)  $\times$   $10.0\ \text{cm}$  (width)  $\times$   $30.0\ \text{cm}$  (height) is placed in the optical setup containing a mixture of clean water ( $1000\ \text{ml}$ ) and milk. Different volumes of milk, i.e.,  $1\ \text{ml}$ ,  $2\ \text{ml}$  and  $3\ \text{ml}$ , are individually used in experiments to emulate different levels of water turbidity. Experimental results of the complex-field reconstruction are shown in Figs. 4(a)–4(f), and the object is Group 2 Element 6 of USAF 1951 resolution target. Despite an increase in water turbidity, the horizontal bars can be clearly observed and distinguished. To illustrate the resolvability, the pixels along the line in Fig. 3(a) are extracted and shown in Figs. 4(g) and 4(h). The peaks and troughs demonstrate that Group 2 Element 6 is well resolved. The CNRs of the reconstructed amplitude patterns in Figs. 4(a)–4(c) are  $7.02$ ,  $5.33$  and  $5.30$ , respectively. It is demonstrated that the proposed method can realize high-quality complex-field reconstruction in turbid water environments.

The proposed method is further applied to realize high-quality complex-field reconstruction of a biological sample through scattering media. A dragonfly wing is used as the target which is primarily composed of membranes and veins. Single-pixel light intensities are collected through a diffuser (Thorlabs, DG10-1500), and reconstruction results are shown in Fig. 5. The reconstructed amplitude pattern in Fig. 5(a) renders clear distribution of veins and membranes, and Fig. 5(b) shows a retrieved phase pattern. The variation of spatial distribution in different regions of the dragonfly wing is clearly distinguished. The reconstructed complex field is consistent with biological structure of a dragonfly wing. It is experimentally demonstrated that the proposed method is feasible and promising to be used for biological imaging through scattering media. As biological imaging through scattering media is challenging due to the complex nature of thick tissues, the proposed method offers a promising solution to visualizing



complex biological structures in challenging conditions.

**Fig. 5.** Experimental results obtained when a dragonfly wing is used as a sample and tested through a diffuser: (a) a reconstructed amplitude pattern, and (b) a retrieved phase pattern.

The experimental results in Figs. 3–5 have a size of  $128 \times 128$  pixels, and the unwrapped phase patterns are obtained by using Goldstein's branch cut algorithm [25]. A sampling ratio of 200% is used in this study. In fact, the smallest sampling ratio of 400% is theoretically necessary for high-quality reconstruction [26]. Therefore, the proposed method has successfully reduced the sampling ratio by 50%. The proposed method can facilitate the realization of high-quality complex-field reconstruction using a low sampling ratio. The experimental results are also obtained under different sampling ratios (see Fig. S2 in Supplement 1), indicating that a sampling ratio of 200% is sufficient when the proposed method is applied. In addition, the convergence speed of the proposed reconstruction algorithm is also shown in Figs. S3 and S4 in Supplement 1. Compared to the existing SPI approaches [27,28], the proposed method has been developed to reconstruct high-quality complex fields and effectively overcome the challenges in recovering high-quality phase information through scattering media.

In conclusion, complex-field imaging through scattering media with single-pixel detection has been reported, and high-quality amplitude and phase patterns are retrieved. A novel AP algorithm has been developed for complex-field reconstruction using the collected single-pixel light intensities. The momentum and denoising are flexibly integrated to enhance the convergence speed and reduce the sampling ratio with an enhancement of reconstruction quality. The developed single-pixel complex-field imaging through scattering media has been experimentally verified, and the retrieved complex fields are of high quality. It is expected that the proposed method can be promising for high-

quality complex-field imaging through various scattering media (e.g., placed before the object), and can provide a solution for high-quality structural visualization of various samples in scattering environments.

**Funding.** Hong Kong Research Grants Council (15224921, 15223522); The Hong Kong Polytechnic University (1-WZ4M, 1-CDJA).

**Disclosures.** The authors declare no conflicts of interest.

**Data Availability.** Data underlying the results presented in this paper are not publicly available at this time but may be obtained from the authors upon reasonable request.

## REFERENCES

1. E. Hecht, *Optics*, 5th ed. (Pearson, 2017).
2. Y. Park, C. Depeursinge, and G. Popescu, *Nat. Photonics* **12**, 578 (2018).
3. J. C. Dainty and J. R. Fienup, in *Image Recovery: Theory and Application*, H. Stark, ed. (Academic, 1987), pp. 231–275.
4. R. P. Millane, *J. Opt. Soc. Am. A* **7**, 394 (1990).
5. I. McNulty, J. Kirz, C. Jacobsen, E. H. Anderson, M. R. Howells, and D. P. Kern, *Science* **256**, 1009 (1992).
6. G. J. Williams, H. M. Quiney, B. B. Dhal, C. Q. Tran, K. A. Nugent, A. G. Peele, D. Paterson, and M. D. de Jonge, *Phys. Rev. Lett.* **97**, 025506 (2006).
7. J. W. Goodman, *Speckle Phenomena in Optics: Theory and Applications* (Roberts & Company Publishers, 2007).
8. I. M. Vellekoop and A. P. Mosk, *Opt. Lett.* **32**, 2309 (2007).
9. R. Tyson, *Principles of Adaptive Optics* (CRC Press, 2010).
10. O. Katz, P. Heidmann, M. Fink, and S. Gigan, *Nat. Photonics* **8**, 784 (2014).
11. M. P. Edgar, G. M. Gibson, and M. J. Padgett, *Nat. Photonics* **13**, 13 (2019).
12. M. F. Duarte, M. A. Davenport, D. Takhar, J. N. Laska, T. Sun, K. F. Kelly, and R. G. Baraniuk, *IEEE Signal Process. Mag.* **25**, 83 (2008).
13. Z. Zhang, X. Ma, and J. Zhong, *Nat. Commun.* **6**, 6225 (2015).
14. Y. Hao, Y. Xiao, and W. Chen, *Opt. Express* **31**, 14389 (2023).
15. W. Chen, B. Javidi, and X. Chen, *Adv. Opt. Photon.* **6**, 120 (2014).
16. D. Shrekenhamer, C. M. Watts, and W. J. Padilla, *Opt. Express* **21**, 12507 (2013).
17. L. Zhou, Y. Xiao, and W. Chen, *Opt. Express* **31**, 23027 (2023).
18. R. W. Gerchberg and W. O. Saxton, *Optik* **35**, 237 (1972).
19. J. W. Goodman, *Introduction to Fourier Optics* (McGraw-Hill, 1996).
20. A. Maiden, D. Johnson, and P. Li, *Optica* **4**, 736 (2017).
21. B. Redding, M. A. Choma, and H. Cao, *Nat. Photonics* **6**, 355 (2012).
22. Y. Peng and W. Chen, *APL Machine Learning* **2**, 036114 (2024).
23. Q. Song, Q. H. Liu, and W. Chen, *Appl. Phys. Lett.* **124**, 211104 (2024).
24. H. T. Chandran, R. Ma, Z. Xu, J. C. Veetil, Y. Luo, T. A. Dela Peña, I. Gunasekaran, S. Mahadevan, K. Liu, Y. Xiao, H. Xia, J. Wu, M. Li, S.-W. Tsang, X. Yu, W. Chen, and G. Li, *Adv. Mater.* **36**, 2407271 (2024).
25. R. M. Goldstein, H. A. Zebker, and C. L. Werner, *Radio Sci.* **23**, 713 (1988).
26. A. Conca, D. Edidin, M. Hering, and C. Vinzant, *Appl. Comput. Harmon. Anal.* **38**, 346 (2015).
27. W. Wang, X. Hu, J. Liu, S. Zhang, J. Suo, and G. Situ, *Opt. Express* **23**, 28416 (2015).
28. G. M. Gibson, S. D. Johnson, and M. J. Padgett, *Opt. Express* **28**, 28190 (2020).

## References with full titles

1. E. Hecht, *Optics*, 5th ed. (Pearson, 2017).
2. Y. Park, C. Depeursinge, and G. Popescu, "Quantitative phase imaging in biomedicine," *Nat. Photonics* **12**, 578–589 (2018).
3. J. C. Dainty and J. R. Fienup, "Phase retrieval and image reconstruction for astronomy," in *Image Recovery: Theory and Application*, H. Stark, ed. (Academic, 1987), pp. 231–275.
4. R. P. Millane, "Phase retrieval in crystallography and optics," *J. Opt. Soc. Am. A* **7**, 394–411 (1990).
5. I. McNulty, J. Kirz, C. Jacobsen, E. H. Anderson, M. R. Howells, and D. P. Kern, "High-resolution imaging by Fourier transform X-ray holography," *Science* **256**, 1009–1012 (1992).
6. G. J. Williams, H. M. Quiney, B. B. Dhal, C. Q. Tran, K. A. Nugent, A. G. Peele, D. Paterson, and M. D. de Jonge, "Fresnel coherent diffractive imaging," *Phys. Rev. Lett.* **97**, 025506 (2006).
7. J. W. Goodman, *Speckle Phenomena in Optics: Theory and Applications* (Roberts & Company Publishers, 2007).
8. I. M. Vellekoop and A. P. Mosk, "Focusing coherent light through opaque strongly scattering media," *Opt. Lett.* **32**, 2309–2311 (2007).
9. R. Tyson, *Principles of Adaptive Optics* (CRC Press, 2010).
10. O. Katz, P. Heidmann, M. Fink, and S. Gigan, "Non-invasive single-shot imaging through scattering layers and around corners via speckle correlations," *Nat. Photonics* **8**, 784–790 (2014).
11. M. P. Edgar, G. M. Gibson, and M. J. Padgett, "Principles and prospects for single-pixel imaging," *Nat. Photonics* **13**, 13–20 (2019).
12. M. F. Duarte, M. A. Davenport, D. Takhar, J. N. Laska, T. Sun, K. F. Kelly, and R. G. Baraniuk, "Single-pixel imaging via compressive sampling," *IEEE Signal Process. Mag.* **25**, 83–91 (2008).
13. Z. Zhang, X. Ma, and J. Zhong, "Single-pixel imaging by means of Fourier spectrum acquisition," *Nat. Commun.* **6**, 6225 (2015).
14. Y. Hao, Y. Xiao, and W. Chen, "High-fidelity ghost diffraction through complex scattering media using a modified Gerchberg-Saxton algorithm," *Opt. Express* **31**, 14389–14402 (2023).
15. W. Chen, B. Javidi, and X. Chen, "Advances in optical security systems," *Adv. Opt. Photon.* **6**, 120–155 (2014).
16. D. Shrekenhamer, C. M. Watts, and W. J. Padilla, "Terahertz single pixel imaging with an optically controlled dynamic spatial light modulator," *Opt. Express* **21**, 12507–12518 (2013).
17. L. Zhou, Y. Xiao, and W. Chen, "High-resolution self-corrected single-pixel imaging through dynamic and complex scattering media," *Opt. Express* **31**, 23027–23039 (2023).
18. R. W. Gerchberg and W. O. Saxton, "A practical algorithm for the determination of the phase from image and diffraction plane pictures," *Optik* **35**, 237 (1972).
19. J. W. Goodman, *Introduction to Fourier Optics* (McGraw-Hill, 1996).
20. A. Maiden, D. Johnson, and P. Li, "Further improvements to the ptychographical iterative engine," *Optica* **4**, 736–745 (2017).
21. B. Redding, M. A. Choma, and H. Cao, "Speckle-free laser imaging using random laser illumination," *Nat. Photonics* **6**, 355–359 (2012).
22. Y. Peng and W. Chen, "Dual-modality ghost diffraction in a complex disordered environment using untrained neural networks," *APL Machine Learning* **2**, 036114 (2024).
23. Q. Song, Q. H. Liu, and W. Chen, "High-resolution ghost imaging through dynamic and complex scattering media with adaptive moving average correction," *Appl. Phys. Lett.* **124**, 211104 (2024).
24. H. T. Chandran, R. Ma, Z. Xu, J. C. Veetil, Y. Luo, T. A. Dela Peña, I. Gunasekaran, S. Mahadevan, K. Liu, Y. Xiao, H. Xia, J. Wu, M. Li, S.-W. Tsang, X. Yu, W. Chen, and G. Li, "High-detectivity all-polymer photodiode empowers smart vitality surveillance and computational imaging rivaling silicon diodes," *Adv. Mater.* **36**, 2407271 (2024).
25. R. M. Goldstein, H. A. Zebker, and C. L. Werner, "Satellite radar interferometry: two-dimensional phase unwrapping," *Radio Sci.* **23**, 713–720 (1988).
26. A. Conca, D. Edidin, M. Hering, and C. Vinzant, "An algebraic characterization of injectivity in phase retrieval," *Appl. Comput. Harmon. Anal.* **38**, 346–356 (2015).
27. W. Wang, X. Hu, J. Liu, S. Zhang, J. Suo, and G. Situ, "Gerchberg-Saxton-like ghost imaging," *Opt. Express* **23**, 28416–28422 (2015).
28. G. M. Gibson, S. D. Johnson, and M. J. Padgett, "Single-pixel imaging 12 years on: a review," *Opt. Express* **28**, 28190–28208 (2020).